

## PROSPECTS FOR DELENSING THE COSMIC MICROWAVE BACKGROUND FOR STUDYING INFLATION

GABRIELLE SIMARD, DUNCAN HANSON AND GIL HOLDER  
Department of Physics, McGill University, Montreal, Quebec H3A 2T8, Canada  
*Draft version January 27, 2023*

## ABSTRACT

The recent BICEP2 measurement of excess B-mode polarization on large scales allows the possibility of measuring not only the amplitude of these fluctuations but also the scale dependence, which can be parametrized as the tensor spectral index. Measurements of this scale dependence will be hindered by the secondary B-mode polarization anisotropy induced by gravitational lensing. Fortunately, these contaminating B modes can be estimated and removed with a sufficiently good estimate of the intervening gravitational potential and a good map of CMB E-mode polarization. We present forecasts for how well these gravitational lensing B modes can be removed, assuming that the lensing potential can be estimated either internally from CMB data or using maps of the cosmic infrared background as a tracer. We find that maps of the cosmic infrared background are more effective for delensing at the noise levels of the current generation of CMB experiments, while the CMB maps themselves will ultimately be best for delensing when the experiments have sufficient sensitivity to measure the tensor spectral index to an accuracy of 0.02 or better. This level is particularly interesting, as it corresponds to the spectral index predicted by the consistency relation for single-field slow-roll models of inflation with  $r = 0.2$ .

## 1. INTRODUCTION

The recent BICEP2 high-sensitivity measurements of B-mode polarization in the microwave sky on large angular scales ( $\ell \lesssim 300$ ) have generated a great deal of excitement (BICEP2 Collaboration 2014b). Many have interpreted this measurement as the imprint of gravitational radiation from the epoch of inflation (see for example, BICEP2 Collaboration 2014b and Martin et al. 2014, for a review of different models); others have understood the signal as the signature of alternatives to inflation (Brandenberger et al. 2014; Gerbino et al. 2014; Wang & Xue 2014; Cai et al. 2014), topological defects (Lizarraga et al. 2014; Moss & Pogosian 2014) or even Galactic dust (Planck Collaboration Int. XXX 2014; Flauger et al. 2014; Mortonson & Seljak 2014).

Regardless of the origin of the signal, it would be interesting to probe its scale dependence. In this paper, we investigate the prospects for measuring this scale dependence (henceforth called “tensor tilt”) of the tensor fluctuations using future polarization measurements. Fig. 1 shows the effect of varying the tensor tilt  $n_T$  on the theoretical power spectrum of the primordial B modes for a fixed value of the tensor-to-scalar ratio  $r$ . The  $r = 0.2$  power spectra have been normalized at  $\ell = 100$ , an angular scale well probed by the BICEP2 experiment, although for the results presented in Section 3 the pivot scale at which  $r$  is taken will be held to  $k_0 = 0.002 \text{ Mpc}^{-1}$ . This choice of pivot scale affects the quoted values of  $r$  but not the r-marginalized constraints on  $n_T$  (Boyle et al. 2014).

A serious impediment to measuring the tensor tilt will be noise coming from gravitational lensing of the CMB polarization fluctuations generated by scalar fluctuations. Removing this signal is possible, using a procedure known as “delensing” (Knox & Song 2002; Kesden et al. 2002). In principle, with sufficiently high signal-to-

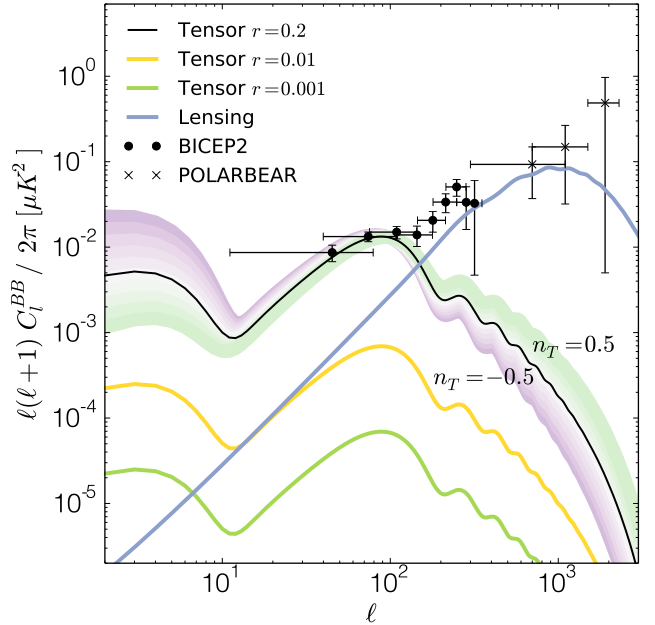


FIG. 1.— Theoretical power spectrum of the gravitational waves B-mode polarization and lensing B-mode polarization along with the BICEP2 (BICEP2 Collaboration 2014b) and POLARBEAR (POLARBEAR Collaboration 2014a) measurements. The shaded region illustrates the tilt imprinted on a  $r = 0.2$  primordial power spectrum from  $n_T = -0.5$  (purple) to  $n_T = 0.5$  (green). All tensor power spectra are for  $r$  defined at  $\ell = 100$ .

noise measurements and in the absence of any primordial B-mode signal this delensing procedure can be done with arbitrarily high precision (Seljak & Hirata 2004). The ability to remove the lensing signal requires a good map of the polarization fluctuations from the scalars (E-mode polarization anisotropies) and a good estimate of the intervening projected gravitational potential. E-mode polarization maps can be obtained only from sensitive CMB polarization measurements on the relevant angu-

lar scales, while the gravitational potential can either be estimated from the CMB data or obtained using astronomical sources as tracers of the potential.

The paper is divided as follow: in Sect. 2 we quantify the noise levels associated with these tracers of the lensing potential and E modes and describe the forecasting method used to delens the B-mode power. In Sect. 3 we present the resulting constraints and our conclusions are summarized in Sect. 4.

Throughout this work, we use the Planck/WP/highL fiducial cosmology (Planck Collaboration XVI 2014) for all cosmological parameters except  $r$  and  $n_T$ . We take the fiducial values of the tensor power spectrum parameters to follow the consistency relation  $n_T = -r/8$ , characteristic of the single-field slow-roll inflation models (Liddle & Lyth 1992). The CMB temperature, CMB polarization and lensing potential power spectrum have been computed using the CLASS Boltzmann code (Blas et al. 2011).

## 2. FORECASTING METHOD

We discuss here the tools we used to achieve CMB delensing and to compute forecasted errors on the parameters describing the primordial B modes. Gravitational lensing deflects CMB temperature and polarization primordial anisotropies according to (Lewis & Challinor 2006):

$$T^{\text{len}}(\hat{\mathbf{n}}) = T^{\text{unl}}(\hat{\mathbf{n}} + \nabla\phi(\hat{\mathbf{n}})) \quad (1)$$

$$(Q \pm iU)^{\text{len}}(\hat{\mathbf{n}}) = (Q \pm iU)^{\text{unl}}(\hat{\mathbf{n}} + \nabla\phi(\hat{\mathbf{n}})). \quad (2)$$

The lensing potential  $\phi(\hat{\mathbf{n}})$  can be expressed as a line-of-sight integral:

$$\phi(\hat{\mathbf{n}}) = -2 \int_0^{z_{\text{rec}}} \frac{dz}{H(z)} \Psi(z, D(z) \hat{\mathbf{n}}) \quad (3)$$

$$\times \left( \frac{1}{D(z)} - \frac{1}{D(z_{\text{rec}})} \right),$$

where  $H(z)$  is the Hubble factor,  $\Psi(z, \mathbf{x})$  the Newtonian gravitational potential and  $D(z)$  the comoving distance to the redshift  $z$ . A flat universe has been assumed in writing expression (3). Rewriting the right-hand side of equation (1) in the E modes and B modes CMB polarization formalism (Zaldarriaga & Seljak 1997) and expanding it up to first order in the lensing potential, we get the following approximation for the lensed B modes (Hu 2000):

$$B_{\ell m}^{\text{len}} \approx B_{\ell m}^{\text{unl}} \quad (4)$$

$$+ \sum_{\ell' m'} \sum_{LM} f_{\ell \ell' L} E_{\ell' m'}^{\text{unl}*} \begin{pmatrix} \ell & \ell' & L \\ m & m' & M \end{pmatrix} \phi_{LM}^*.$$

The  $f_{\ell \ell' L}$  couplings are given by

$$f_{\ell \ell' L} = \frac{F_{\ell \ell' L}^{-2} - F_{\ell \ell' L}^2}{2i}, \quad (5)$$

where

$$F_{\ell \ell' L}^s = \frac{1}{2} [-\ell(\ell+1) + \ell'(\ell'+1) + L(L+1)] \quad (6)$$

$$\times \sqrt{\frac{(2\ell+1)(2\ell'+1)(2L+1)}{4\pi}} \begin{pmatrix} \ell & \ell' & L \\ -s & s & 0 \end{pmatrix}.$$

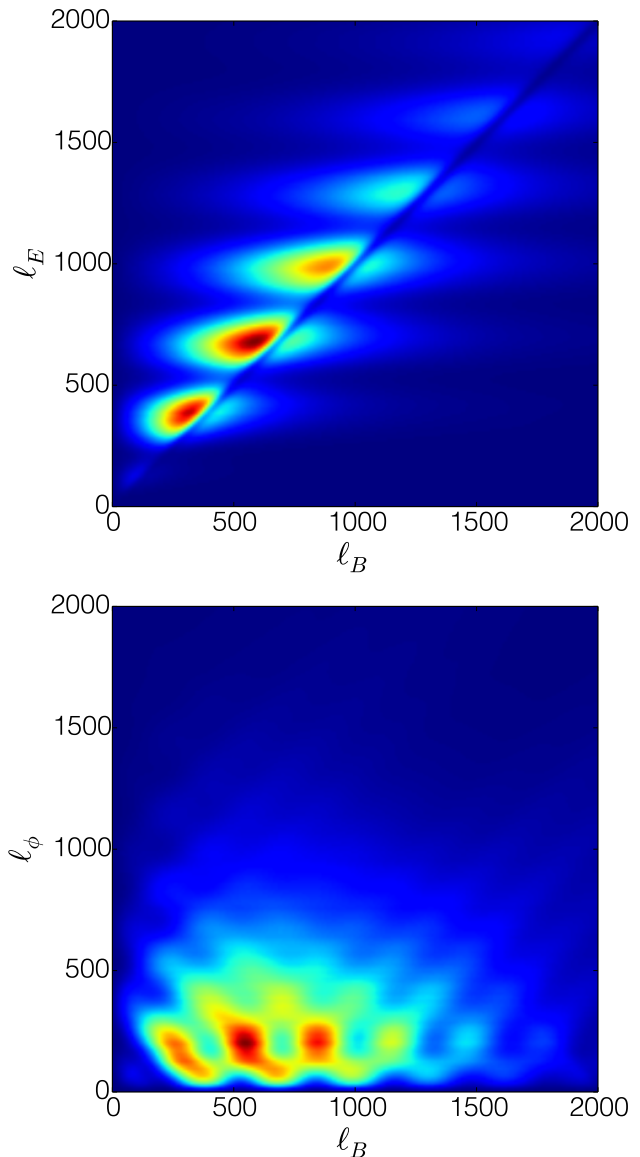


FIG. 2.— Source terms for the lensed B modes. We have plotted  $\ell_B (\partial C_{\ell_B}^B / \partial C_{\ell_X}^X) C_{\ell_X}^X$  where  $X \in \{E, \phi\}$  such that the colour along each column gives the fraction contribution per multipole to the lensed B modes from the corresponding source. The lensing B modes at  $\ell_B = 600$ , for example, are sourced largely by contributions from the lensing potential at  $\ell_\phi \approx 175$  and  $\ell_E \approx 650$ . Delensing can be performed if one has measurements of these two fields in the corresponding multipole ranges.

Taking the power spectrum of equation (4), we obtain:

$$C_\ell^{\text{B, len}} = C_\ell^{\text{B, unl}} + \frac{1}{2\ell+1} \sum_{\ell' L} |f_{\ell \ell' L}|^2 C_{\ell'}^{\text{E, unl}} C_L^\phi. \quad (7)$$

It is useful to gain an intuitive understanding of which scales in E-mode polarization and the lensing potential source the lensing B modes. For this purpose, in Fig. 2, we have plotted the kernel for the lensing B-mode power spectrum, broken into contributions from  $C_\ell^{\text{E, unl}}$  and  $C_L^\phi$ . It can be seen that in general the important E modes contributing to a given  $\ell$  in lensing B modes are those from a scale that is just slightly smaller (larger in  $\ell$ ). Thus, to delens B modes up to  $\ell \sim 500$  it is only required to accurately measure E modes up to  $\ell \sim 1000$ ,

given a good map of the gravitational potential. Obtaining accurate E-mode measurements on these scales is relatively straightforward: current ground-based CMB experiments such as SPTpol (Austermann et al. 2012), ACTpol (Niemack et al. 2010), and PolarBear (Kermish et al. 2012) make sample-variance limited measurements of the E-mode polarization on these scales.

For the lensing potential, most of the lensing B modes are generated by gravitational potential fluctuations on half-degree scales or larger ( $\ell \lesssim 500$ ). There are again a number of possible tracers for these modes. CMB lensing measurements can be used, although polarization-based lensing measurements require high sensitivity and sensitivity to smaller angular scales than are required for large-scale tensor B-mode experiments (such as BI-CEP2). Alternatively, astrophysical tracers could be used to estimate the potential, provided they are sufficiently correlated with the lensing potential.

The idea behind delensing is to build a noisy estimate of the lensing B modes using Wiener-filtered E modes and lensing potential  $\phi$ . This estimate is then subtracted from the perfectly reconstructed B modes, leaving as a difference the residual B modes:

$$C_\ell^{\text{B,res}} = \frac{1}{2\ell + 1} \sum_{\ell_1 \ell_2} |f_{\ell \ell_1 \ell_2}|^2 \left[ C_{\ell_1}^{\text{E,len}} C_{\ell_2}^\phi - \left( \frac{(C_{\ell_1}^{\text{E,len}})^2}{C_{\ell_1}^{\text{E,len}} + N_{\ell_1}^{\text{E}}} \right) \left( \frac{(C_{\ell_2}^\phi)^2}{C_{\ell_2}^\phi + N_{\ell_2}^\phi} \right) \right]. \quad (8)$$

A formal derivation of this expression can be found in Smith et al. 2009. In writing equation (8), we have substituted the *unlensed* E-mode power spectrum coming from the derivation of equation (7) by the *lensed* E-mode power spectrum, which has been shown by Lewis et al. 2011 to produce an estimated lensed B-mode power spectrum effectively accurate to higher order. The experimental noise power spectrum can be written as (Knox 1995):

$$N_\ell^{\text{E}} = N_\ell^{\text{B}} = \Delta_P^2 \exp\left(\frac{\ell(\ell+1)\theta_{\text{FWHM}}^2}{8 \ln 2}\right), \quad (9)$$

where  $\Delta_P$  is the polarization pixel noise in [ $\mu\text{K-radian}$ ] and  $\theta_{\text{FWHM}}$  is the full-width at half-maximum of the beam, assuming this beam is Gaussian. We do not consider an additional foreground noise power spectrum, making this forecast optimistic.

The lensing reconstruction noise power spectrum  $N_\ell^\phi$  can be obtained through the prevalent quadratic estimator method (Hu 2000). This technique builds an estimate of the lensing potential from the optimally filtered off-diagonal correlations between two lensed CMB fields  $X, X' \in \{T, E, B\}$ . We use the EB estimator which yields the best signal to noise ratio at high experimental sensitivities. The resulting quadratic lens reconstruction

noise level can be expressed as (Okamoto & Hu 2003):

$$N_\ell^\phi = \left[ \frac{1}{2\ell + 1} \sum_{\ell_1 \ell_2} |f_{\ell \ell_1 \ell_2}^{\text{EB}}|^2 \right] \times \left( \frac{1}{C_{\ell_1}^{\text{B,len}} + N_{\ell_1}^{\text{B}}} \right) \left( \frac{(C_{\ell_2}^{\text{E,len}})^2}{C_{\ell_2}^{\text{E,len}} + N_{\ell_2}^{\text{E}}} \right)^{-1}. \quad (10)$$

We used the fast real-space algorithm proposed by Smith et al. (2012) to compute the geometrical factors described in equations (5) and (6) necessary for the numerical implementation of equations (8) and (10).

It can be seen from equation (10) that the lensing B modes act as a contaminant for the lensing reconstruction process. Substituting the signal+noise lensed B modes of equation (10) by delensed B modes, defined in this forecast as

$$C_\ell^{\text{B,del}} \approx C_\ell^{\text{B,unl}} + C_\ell^{\text{B,res}} + N_\ell^{\text{B}}, \quad (11)$$

one can estimate the lensing potential with higher signal-to-noise and then produce lower residual B modes. Repeating these steps until convergence of  $C_\ell^{\text{B,del}}$  is referred to as iterative delensing (Smith et al. 2009; Seljak & Hirata 2004). Quadratic delensing will indicate the use of a delensed power spectrum  $C_\ell^{\text{B,del}}$  computed through only one iteration.

Lensing reconstruction can also be achieved using large-scale structure (Smith et al. 2012). We explore here the possibility of estimating the lensing potential by using its cross-correlation with the CIB, its best known tracer. The CIB is an extragalactic radiation field generated by the unresolved emission from star-forming galaxies. It is generated by dust which is heated by the UV light from young stars and then reradiates thermally in the infrared with a graybody spectrum of  $T \sim 30\text{K}$ . Due to its larger temperature, fluctuations in the CIB dominate over the CMB on most angular scales at frequencies  $\nu \gtrsim 300\text{GHz}$ . The CIB contains approximately half of the total extragalactic stellar flux, and has long been predicted to have excellent redshift overlap with the CMB lensing potential (Song et al. 2003). Recent measurements of the cross-correlation between the lensing potential and high signal-to-noise measurements of the CIB fluctuations from the *Planck* and *Herschel* satellites have upheld these predictions (POLARBEAR Collaboration 2014b; Planck Collaboration XVIII 2014; Hanson et al. 2013; Holder et al. 2013).

In this work, we assume that such measurements of the CIB are available, and that the cross-correlation between the CIB and the lensing potential can be well-approximated as flat with a constant correlation coefficient

$$f_{\text{corr}} = \frac{C_\ell^{\text{CIB} \times \phi}}{\sqrt{C_\ell^\phi C_\ell^{\text{CIB}}}}. \quad (12)$$

This simple approximation is quite accurate (see for example Fig. 13 of Planck Collaboration XVIII 2014). Including the Poisson noise component to the CIB power spectrum in equation (12) causes  $f_{\text{corr}}$  to fall off on small scales, but on scales larger than  $\ell \sim 500$  of interest for delensing, the flatness of the correlation factor is not substantially affected. Although recent measurements have

shown a correlation at the  $f_{\text{corr}} = 0.8$  level, we will pessimistically also consider delensing with correlation coefficients as low as  $f_{\text{corr}} = 0.4$ . This could effectively be the case, for example, in a region with comparable foreground and CIB power. The introduction of this correlation coefficient results in a simple expression for the lensing estimate signal+noise power spectrum used in Eq. (8);

$$C_\ell^\phi + N_\ell^\phi = C_\ell^\phi / f_{\text{corr}}^2. \quad (13)$$

Assuming Gaussianity of the likelihood function  $\mathcal{L}(\mathbf{d}|\boldsymbol{\theta})$  which gives the probability distribution of a cosmological model  $\boldsymbol{\theta}$  given some set of independent observations  $\mathbf{d}$ , we use the Fisher matrix formalism to compute forecasted errors on the tensor tilt. For the present analysis, the data covariance matrix will be reduced to the B-modes power spectrum since the constraining power on cosmological parameters such as  $r$  and  $n_T$  comes mainly from the B-mode signal. Each element of the Fisher matrix reduces to (Jungman et al. 1996)

$$F_{ij} = \sum_{\ell_{\min}}^{\ell_{\max}} \frac{(C_\ell^{\text{B}})_{,i} (C_\ell^{\text{B}})_{,j}}{(\delta C_\ell^{\text{B}})^2}, \quad (14)$$

where the expected  $1\sigma$  error on the measurement of the B-modes power spectrum is

$$\delta C_\ell^{\text{B}} = \sqrt{\frac{2}{(2\ell + 1) f_{\text{sky}}}} C_\ell^{\text{B}}. \quad (15)$$

The marginalized error on a given parameter of the model corresponds to  $\sigma(\theta_i) = \sqrt{(F^{-1})_{ii}}$ .

### 3. CONSTRAINTS ON TENSOR TILT

We have computed the projected constraint on the tensor tilt assuming different delensing scenarios; results are shown in Fig. 3. The two limiting cases correspond to a situation where no lensing B modes are removed (solid orange curves) and where the total B modes include no lensing B modes (solid light gray curves). The solid and dotted dark gray curves correspond to quadratic and iterative CMB delensing and the shaded regions correspond to delensing using the CIB, where the correlation factor  $f_{\text{corr}}$  is comprised between 0.4 and 0.8. For simplicity we will consider that the E-mode estimate and the lensing potential estimate are obtained through the same CMB experiment when considering CMB delensing, which makes the noise power spectra in equations (8) and (10) parametrized by the same beam width and sensitivity. This forecast could be expanded to the case where a large-scale mission is used for the measurement of the E modes and a higher resolution experiment is used for estimating the lensing potential.

The beam width  $\theta_{\text{FWHM}}$  has been fixed to 4 arcmin in both panels; it has been shown that beam size is not an important factor (Boyle et al. 2014; Dodelson 2014; Wu et al. 2014). We have included modes between  $l_{\min} = 10$  and  $l_{\max} = 3000$  in the Fisher matrix calculation, although the large scale cutoff value does not affect significantly the projected constraints on  $n_T$  (Boyle et al. 2014; Dodelson 2014). The sky coverage has been held to  $f_{\text{sky}} = 0.5$ , although for a high resolution experiment the results scale with  $f_{\text{sky}}$  (Dodelson 2014).

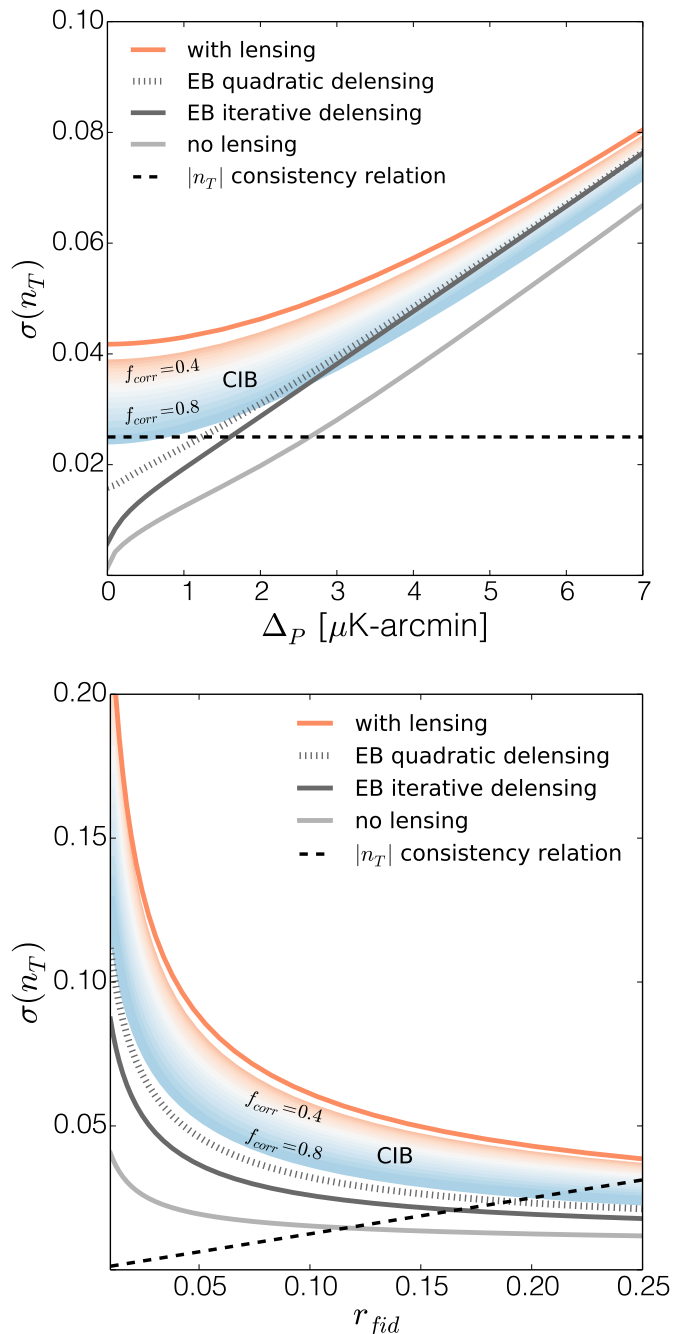


FIG. 3.— *Top panel:* Forecasted constraint on the tensor tilt  $n_T$  marginalized over  $r$  for  $r_{\text{fid}} = 0.2$  and varying polarization sensitivity. *Bottom panel:* Forecasted constraint on the tensor tilt  $n_T$  marginalized over  $r$  for  $\Delta_P = 1 \mu\text{K-arcmin}$  and varying fiducial values of  $r$ . In both panels the black dashed line shows the absolute value of the tensor tilt given it is related to the fiducial value of  $r$  through the consistency relation  $n_T = -r/8$ . The sky coverage has been fixed to  $f_{\text{sky}} = 0.5$  and the beamsize to 4 arcmin in both cases.

The top panel of Fig. 3 shows the forecasted error on  $n_T$  as a function of the polarization experimental noise level. As  $\Delta_P$  approaches 0, no fundamental floor due to the iterative delensing procedure is found, in conformity with previous works (Seljak & Hirata 2004; Smith et al. 2012; Wu et al. 2014). Better than linear improvement on  $\sigma(n_T)$  is observed as polarization noise drops below

$\Delta_P=1 \mu\text{K-arcmin}$  (Caligiuri & Kosowsky 2014).

The error on  $n_T$  depends on the value of  $r$  with which the B-modes power spectrum  $C_\ell^B$  in equations (14) and (15) is computed. This dependence is plotted in the bottom panel of Fig. 3, for a fixed pixel noise of  $\Delta_P=1 \mu\text{K-arcmin}$ . The dashed black line shows the absolute value of  $n_T$ , given that  $n_T$  and  $r$  are related by the consistency relation. It can be seen that going from  $r = 0.2$  down to  $r = 0.1$  hinders the ability to distinguish between consistency relation and other models (Caligiuri & Kosowsky 2014; Dodelson 2014).

#### 4. CONCLUSIONS

With sensitive measurements of the polarization of the CMB, it will be possible to probe tensor tilt at a level that is interesting for many inflation models, provided the B modes recently measured by BICEP2 are of inflationary origin. However, what will be required will be sensitivities on the order of  $1 \mu\text{K-arcmin}$  in polarized noise over roughly half the sky. While ambitious, this is exactly the scale that is being considered as Stage-IV CMB experi-

ments like CMB-S4 (Abazajian et al. 2013). CIB-based delensing will be competitive with CMB-based delensing, provided well-correlated CIB maps can be constructed.

#### ACKNOWLEDGMENTS

While this work was being achieved, the preprint of Boyle et al. (2014) was released, which has strong overlaps with the results presented in this paper. GS wishes to thank Ryan Keisler and Elisa G.M. Ferreira for useful discussions and comments. We acknowledge the use of Kendrick Smith's implementation of the Gauss-Legendre quadrature method and of the Wigner-d matrix. GH acknowledges funding from the Canadian Institute for Advanced Research, the National Sciences and Engineering Research Council of Canada and Canada Research Chairs program. DH is supported by the Lorne Trottier Chair in Astrophysics and Cosmology at McGill as well as a CITA National Fellowship. GS acknowledges support from the Fonds de recherche du Québec - Nature et technologies.

#### REFERENCES

- Abazajian, K.N., Arnold, K., Austermann, J., et al. 2013, arXiv:1309.5383
- Austermann, J. E., Aird, K. A., Beall, J. A., et al. 2012, in Society of Photo-Optical Instrumentation Engineers (SPIE) Conference Series, Vol. 8452, Society of Photo-Optical Instrumentation Engineers (SPIE) Conference Series
- BICEP2 Collaboration. 2014b, Phys.Rev.Lett., 112, 241101
- Blas, D., Lesgourgues, J., & Tram, T. 2011, J. Cosmo. Astro. Part. Phys., 7, 034
- Boyle, L., Smith, K. M., Dvorkin, C., & Turok, N. 2014, arXiv:1408.3129
- Brandenberger, R. H., Nayeri, A., & Patil, S. P. 2014, arXiv:1403.4927
- Cai, Y.-F., Quintin, J., Saridakis, E. N., & Wilson-Ewing, E. 2014, J. Cosmo. Astro. Part. Phys., 1407, 033
- Caligiuri, J., & Kosowsky, A. 2014, Phys.Rev.Lett., 112, 191302
- Dodelson, S. 2014, Phys.Rev.Lett., 112, 191301
- Flauger, R., Hill, J. C., & Spergel, D. N. 2014, J. Cosmo. Astro. Part. Phys., 1408, 039
- Gerbino, M., Marchini, A., Pagano, L., et al. 2014, Phys.Rev., D90, 047301
- Hanson, D., Hoover, S., Crites, A., et al. 2013, Phys.Rev.Lett., 111, 141301
- Holder, G., Viero, M., Zahn, O., et al. 2013, Astrophys.J., 771, L16
- Hu, W. 2000, Phys.Rev., D62, 043007
- Jungman, G., Kamionkowski, M., Kosowsky, A., & Spergel, D. N. 1996, Phys.Rev.Lett., 76, 1007
- Kermish, Z. D., Ade, P., Anthony, A., et al. 2012, in Society of Photo-Optical Instrumentation Engineers (SPIE) Conference Series, Vol. 8452, Society of Photo-Optical Instrumentation Engineers (SPIE) Conference Series
- Kesden, M., Cooray, A., & Kamionkowski, M. 2002, Phys.Rev.Lett., 89, 011304
- Knox, L. 1995, Phys.Rev., D52, 4307
- Knox, L., & Song, Y.-S. 2002, Phys.Rev.Lett., 89, 011303
- Lewis, A., & Challinor, A. 2006, Phys.Rept., 429, 1
- Lewis, A., Challinor, A., & Hanson, D. 2011, J. Cosmo. Astro. Part. Phys., 3, 18
- Lizarraga, J., Urrestilla, J., Daverio, D., et al. 2014, Phys.Rev.Lett., 112, 171301
- Liddle, A. R. & Lyth, D. H. 1992, Phys.Lett., B291, 391
- Martin, J., Ringeval, C., Trota, R., & Vennin, V. 2014, arXiv:1405.7272
- Mortonson, M. J., & Seljak, U. 2014, arXiv:1405.5857
- Moss, A., & Pogosian, L. 2014, Phys.Rev.Lett., 112, 171302
- Niemack, M. D., Ade, P., Aguirre, J., et al. 2010, in Society of Photo-Optical Instrumentation Engineers (SPIE) Conference Series, Vol. 7741, Society of Photo-Optical Instrumentation Engineers (SPIE) Conference Series
- Okamoto, T., & Hu, W. 2003, Phys.Rev., D67, 083002
- Planck Collaboration Int. XXX. 2014, arXiv:1409.5738
- Planck Collaboration XVIII. 2014, Astron.Astrophys., in press, arXiv:1303.5078
- Planck Collaboration XVI. 2014, Astron.Astrophys., in press, arXiv:1303.5076
- POLARBEAR Collaboration. 2014a, arXiv:1403.2369
- POLARBEAR Collaboration. 2014b, arXiv:1312.6645
- Seljak, U., & Hirata, C. M. 2004, Phys.Rev., D69, 043005
- Smith, K. M., Cooray, A., Das, S., et al. 2009, AIP Conf.Proc., 1141, 121
- Smith, K. M., Hanson, D., LoVerde, M., Hirata, C. M., & Zahn, O. 2012, J. Cosmo. Astro. Part. Phys., 6, 14
- Song, Y.-S., Cooray, A., Knox, L., & Zaldarriaga, M. 2003, Astrophys.J., 590, 664
- Wang, Y., & Xue, W. 2014, arXiv:1403.5817
- Wu, W., Errard, J., Dvorkin, C., et al. 2014, Astrophys.J., 788, 138
- Zaldarriaga, M., & Seljak, U. 1997, Phys.Rev., D55, 1830